UNIVERSITY OF CAMBRIDGE

Unveiling the Milky Ways Formation History:
Resolving Chemo-Dynamical Substructures in APOGEE and GALAH

Jacob Tutt[1]

[1] Department of Physics, University of Cambridge, UK

Galactic Archaeology's Motivation

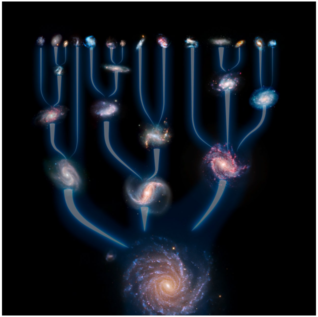

Credit: ESO/L. Calçada

- Uncovering hierarchical galaxy formation.
- Complements higher redshift galaxy formation surveys.
- Probe the ΛCDM model and dark matter distribution.

Merger Type	Number	Mass Ratio
Minor Mergers	$\sim$30	1:3 – 1:100
Major Mergers	$\sim$3	$>$1:3

N-Body Simulations from Fakhouri et al. (2010)

The Era of 'Big Data Astronomy'

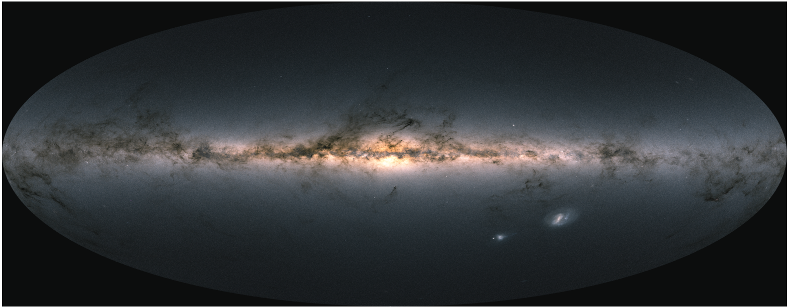

Credit: ESA/Gaia/DPAC, A. Moitinho.

Survey	**Gaia EDR3**	**APOGEE**	**GALAH**
Focus	Astrometry, Photometry	IR spectroscopy	Optical spectroscopy
Sources	$\sim 1.4 \times 10^9$	$\sim$ 734,000	$\sim$ 918,000

The Evolving Picture

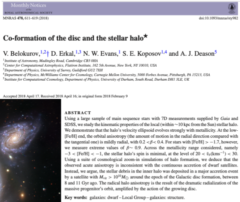

Monthly Notices of the ROYAL ASTRONOMICAL SOCIETY
MNRAS **478,** 611–619 (2018) doi:10.1093/mnras/sty982

Co-formation of the disc and the stellar halo★

V. Belokurov,[1,2]† D. Erkal,[1,3] N. W. Evans,[1] S. E. Koposov[1,4] and A. J. Deason[5]
[1] *Institute of Astronomy, Madingley Road, Cambridge CB3 0HA*
[2] *Center for Computational Astrophysics, Flatiron Institute, 162 5th Avenue, New York, NY 10010, USA*
[3] *Department of Physics, University of Surrey, Guildford GU2 7XH*
[4] *Department of Physics, McWilliams Center for Cosmology, Carnegie Mellon University, 5000 Forbes Avenue, Pittsburgh, PA 15213, USA*
[5] *Institute for Computational Cosmology, Department of Physics, University of Durham, South Road, Durham DH1 3LE, UK*

Accepted 2018 April 17. Received 2018 April 16; in original form 2018 February 9

ABSTRACT
Using a large sample of main sequence stars with 7D measurements supplied by *Gaia* and SDSS, we study the kinematic properties of the local (within ~10 kpc from the Sun) stellar halo. We demonstrate that the halo's velocity ellipsoid evolves strongly with metallicity. At the low-[Fe/H] end, the orbital anisotropy (the amount of motion in the radial direction compared with the tangential one) is mildly radial, with $0.2 < \beta < 0.4$. For stars with [Fe/H] > -1.7, however, we measure extreme values of $\beta \sim 0.9$. Across the metallicity range considered, namely $-3 <$ [Fe/H] < -1, the stellar halo's spin is minimal, at the level of $20 < \bar{v}_\theta(\mathrm{kms}^{-1}) < 30$. Using a suite of cosmological zoom-in simulations of halo formation, we deduce that the observed acute anisotropy is inconsistent with the continuous accretion of dwarf satellites. Instead, we argue, the stellar debris in the inner halo was deposited in a major accretion event by a satellite with $M_{vir} > 10^{10} M_\odot$ around the epoch of the Galactic disc formation, between 8 and 11 Gyr ago. The radical halo anisotropy is the result of the dramatic radialization of the massive progenitor's orbit, amplified by the action of the growing disc.

Key words: galaxies: dwarf – Local Group – galaxies: structure.

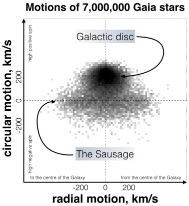

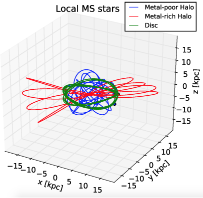

Credit: V. Belokurov et al

Credit: A. Deason (2018)

The GS/E Merger

- Singular massive ($\approx 10^{10} M_\odot$) accretion event $\approx$ (8-10 Gyrs)
- Radial anisotropy in stellar halo's higher metallicities ($-1.7 \leq [Fe/H] \leq -1$)
- Independent α and Al abundance trends
- Contributes $\approx$ 50% of the stellar halo

UNIVERSITY OF CAMBRIDGE

The Evolving Picture

Splash

- Proto-disk population (pre-GS/E)
- Gravitational perturbations of orbits

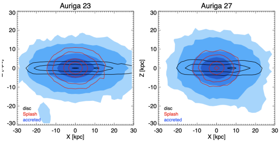

Credit: V. Belokurov et al. (2020)

Eos

- GS/E triggered star formation
- Gas from thick disk and GS/E polluted gas
- Evolves into outer thin disk

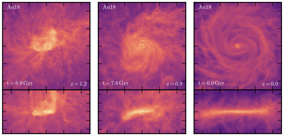

Credit: R. Grand et al. (2020)

Aurora

- Near isotropic velocity distribution
- Ancient pre-disk/ spin-up population
- Rapid star formation/ self-enrichment

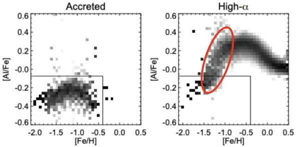

Credit: Belokurov et al. (2022)

Unbiased Detection of Halo Substructures

Goal:

- Unbiased Decomposition of the Milky Way's Halo's (stellar neighbourhood) Substructures.

- **Approach:**
  - Ensure the reproducibility of `Myeong et al.(2022)`.
  - Apply dimensionality reduction to provide insights into clustering stability.
  - Alternative clustering approaches to improve the convergence and computational efficiency.

Integral of Motion Space

Traditional 6D Phase Space:

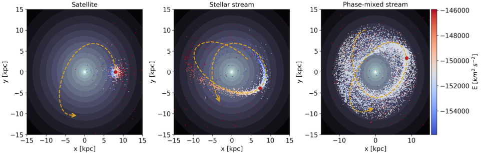

Integrals of Motion:

- Adiabatic invariant
- $\approx$ constant over evolution

For axisymmetric potentials:

Symbol	Description
E	Orbital energy
L_z	Angular momentum (along z-axis)
L	Angular momentum (Total, quasi-conserved)

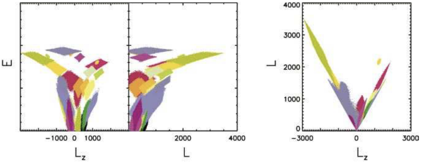

(a) Initial distribution of simulated merger events

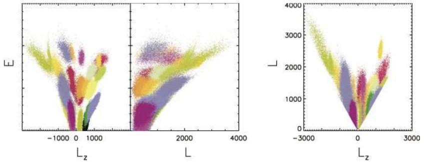

(b) Distribution after 12 Gyr (with observational errors)

Credit: Helmi et al. (2000)

Biases of Halo Selection

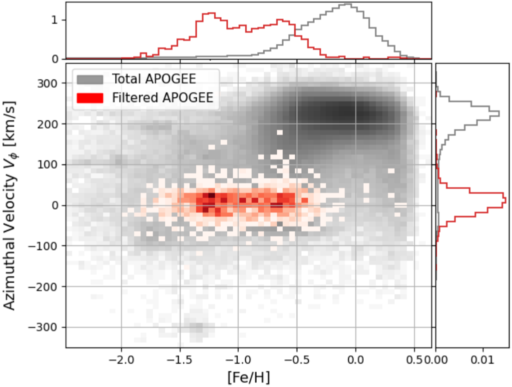

Dynamical Cuts:

- Eccentricity, $e > 0.85$
- Apocenter, > 5kpc
- Energy, $< 0\text{km}^2\text{s}^{-2}$

Chemical Tagging

Credit: Kobayashi et al. (2020)

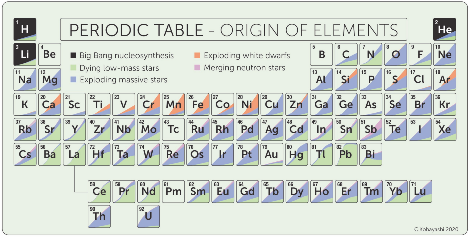

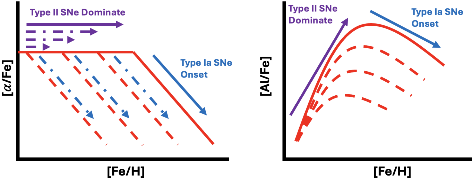

Turn-offs dependent on Star Formation Rate → Host Mass

Insights from Chemical Abundances

- Probe star formation enviroment (ISM)
- Trace nucleosynthetic sources (e.g. SNe, AGB)
- Reflect rates of:
  - Star formation
  - Self-enrichment
- Link to host galaxy mass (IMF)

Data Acquisition

APOGEE

- **Sample Size:** 1612
- **Dimensions:** Energy, [Fe/H], [α/Fe], [Al/Fe], [Ce/Fe], [Mg/Mn]

GALAH

- **Sample Size:** 1061
- **Dimensions:** Energy, [Fe/H], [α/Fe], [Na/Fe], [Al/Fe], [Mn/Fe], [Y/Fe], [Ba/Fe], [Eu/Fe], [Mg/Cu], [Mg/Mn], [Ba/Eu]

Group	Elements	Traces
Iron-peak	Fe, Mn, Ni	Overall Metallicity - Type Ia and II SNe
α-elements	Mg, Si, Ca, Ti	Core-collapse (Type II) SNe
Odd-Z elements	Na, Al	Similar Core-collapse (Type II) SNe
s-process	Y, Ba, Ce	Slow neutron capture - AGB stars
r-process	Eu	Neutron star mergers/ Rare CC-SNe

Dataset Comparison

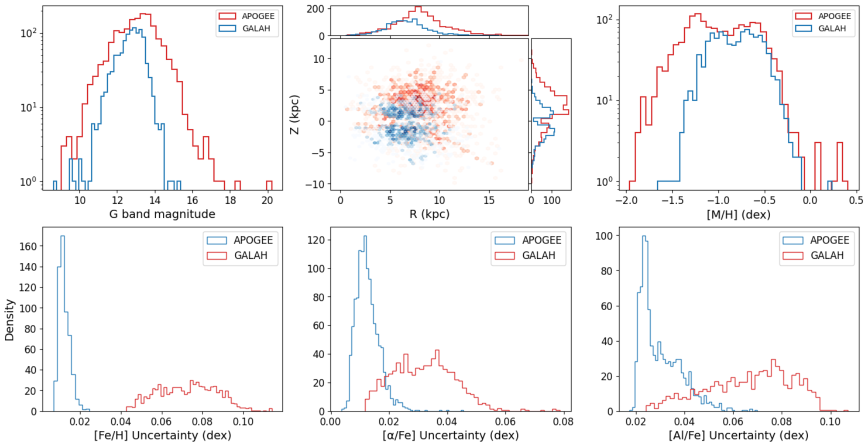

Extreme Deconvolution

The latent distribution of true values $\mathbf{v}$ is modeled as a mixture of K Gaussians:

$$p(\mathbf{v}) = \sum_{j=1}^{K} \alpha_j \mathcal{N}(\mathbf{v} \mid \mathbf{m}_j, \mathbf{V}_j), \tag{1}$$

Likelihoods of noisy observations $\mathbf{w}_i$ are computed by marginalising over $\mathbf{v}$:

$$p(\mathbf{w}_i|\theta) = \sum_j \int d\mathbf{v}\, p(\mathbf{w}_i|\mathbf{v})\, p(\mathbf{v}|j,\theta)\, p(j|\theta). \tag{2}$$

Where:

$$p(\mathbf{w}_i|\mathbf{v}) = \mathcal{N}(\mathbf{w}_i|\mathbf{v}, \mathbf{S}_i), \tag{3}$$

$$p(\mathbf{v}|j,\theta) = \mathcal{N}(\mathbf{v}|\mathbf{m}_j, \mathbf{V}_j), \tag{4}$$

$$p(j|\theta) = \alpha_j. \tag{5}$$

- $\mathbf{w}_i$: observed (noisy) data point
- $\mathbf{v}$: latent true value
- $\mathbf{S}_i$: noise covariance of $\mathbf{w}_i$
- α_j: mixture weight for component j
- $\mathbf{m}_j$: mean of Gaussian component j
- $\mathbf{V}_j$: covariance of component j

Credit: Bovy et al (2011)

Extreme Deconvolution

As a result, the total likelihood of $\mathbf{w}_i$ simplifies to another mixture of Gaussians:

$$p(\mathbf{w}_i|\theta) = \sum_j \alpha_j \mathcal{N}(\mathbf{w}_i \,|\, \mathbf{m}_j, \mathbf{T}_{ij}), \tag{6}$$

where the effective covariance $\mathbf{T}_{ij}$ accounts for both the Gaussian component and the measurement uncertainty:

$$\mathbf{T}_{ij} = \mathbf{V}_j + \mathbf{S}_i. \tag{7}$$

The log-likelihood across all N data points becomes:

$$\phi = \sum_i \ln p(\mathbf{w}_i|\theta) = \sum_i \ln \sum_{j=1}^{K} \alpha_j \mathcal{N}(\mathbf{w}_i \,|\, \mathbf{m}_j, \mathbf{T}_{ij}). \tag{8}$$

Credit: Bovy et al (2011)

Extreme Deconvolution Pipeline

1. **Unbiased component optimisation (AIC/BIC):**

$$\mathrm{AIC} = 2k - 2\ln\mathcal{L}, \quad \mathrm{BIC} = k\ln n - 2\ln\mathcal{L}$$

where:

- k: number of free parameters
- n: number of data points
- $\mathcal{L}$: maximum likelihood

2. **Scaling schemes:**

   2.1 Rescale energy by 10^5 to match other dimensions
   2.2 Standard normal scaling applied to all features

3. **Added functionality to XD:**

   - Automatic probabilistic assignment
   - Automated model selection and initialisation convergence via AIC/BIC

Extreme Deconvolution Pipeline

Motivation of Scaling Scheme

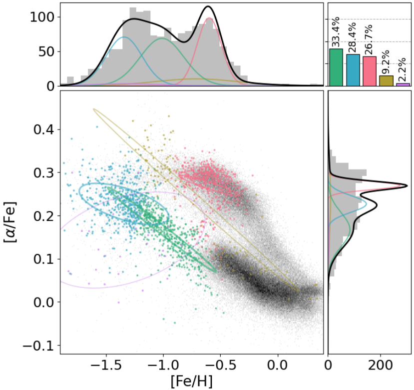

Unscaled XD Clustering Results in [Fe/H] - [α/Fe] Plane

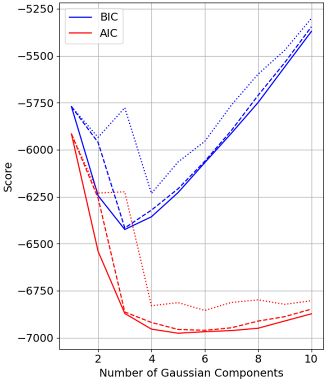

Unscaled XD Clustering Quantitative Model Comparison

Extreme Deconvolution - APOGEE

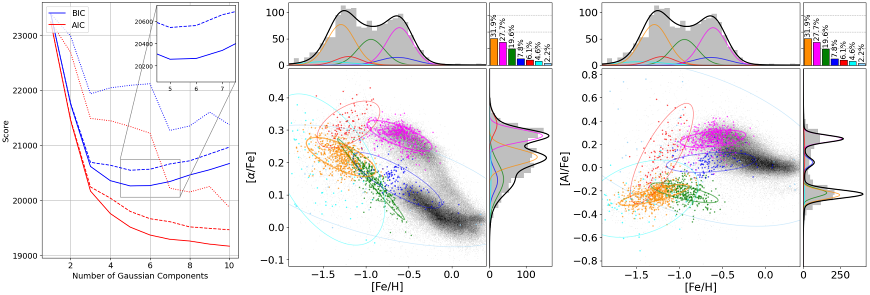

- Subtle BIC Discrepancy with original work (favouring 5 over 7)
- ‘Loss’ of Aurora (Red) Detection in 5 Component Model
- Trivial differences between GS/E (Green/Orange) split

Extreme Deconvolution - GALAH

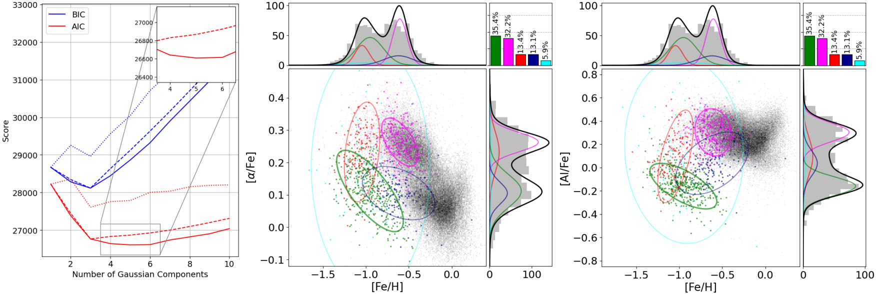

- AIC providing correct isolation of 5 gaussian components
- ‘Exact’ agreement with original work

Key Scientific Recoveries: GS/E Merger

APOGEE

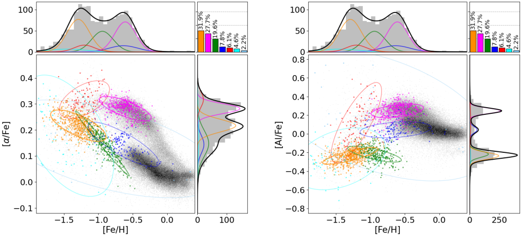

GALAH

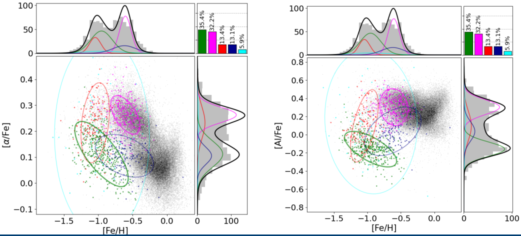

Singular Accreted Component

- Early α knee turnoff
- Low [Al/Fe] turning point
- Trends resembles low mass/ SFR progenitor
- Fractional weighting 51% $\rightarrow$ consistent with `V. Belokurov et al 2018`
- GALAH's high metallicity limit $\rightarrow$ smaller weighting and lack of plateau split

GS/E Eos Aurora Splash

Key Scientific Recoveries: Splash

APOGEE

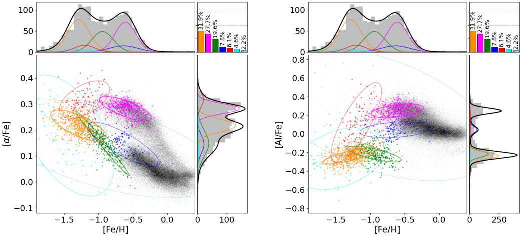

GALAH

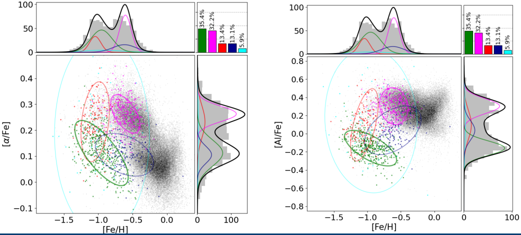

Splash

- Dominant metal rich component ([Fe/H] ≈ -0.7)
- Thick disk like chemistry
- ‘Splashed’ out proto-disk from GS/E

GS/E Eos Aurora Splash

Key Scientific Recoveries: Aurora

APOGEE

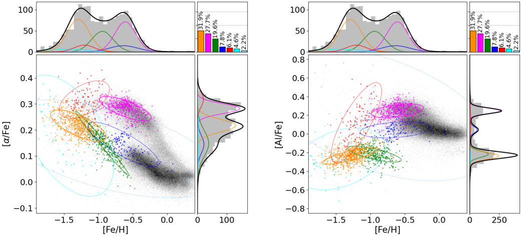

GALAH

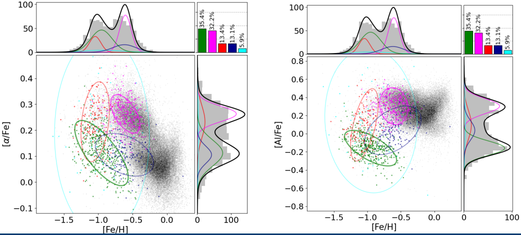

Aurora

- Highly correlated planes: [α/Fe]-[Fe/H] and [Al/Fe]-[Fe/H]
- Ancient rapidly enriching population - early life in a large mass system
- Early pre-disk MW population

GS/E Eos Aurora Splash

Key Scientific Recoveries: Eos

APOGEE

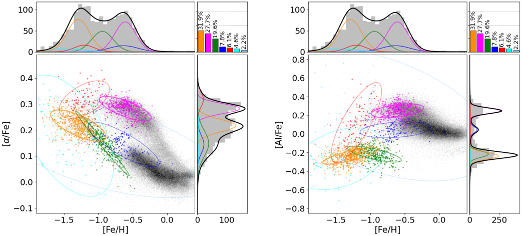

GALAH

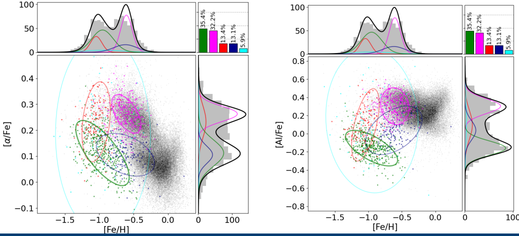

Eos

- Chemically residing between the GS/E population and thin disk
- Born in gas polluted by GS/E merger and thick disk
- Evolves into the thin outer disk

Dimensionality Reduction

Goals:

- Investigate the cohesion and isolation of the substructures identified during high-dimensional clustering
- Understand sensitivity of Aurora's detection.

Dimensionality Reduction

Goals:

- Investigate the cohesion and isolation of the substructures identified during high-dimensional clustering
- Understand sensitivity of Aurora's detection.

UMAP:

- Non-Linear dimensionality reduction
- Advantages over T-SNE:
  - Increased speed
  - Better preservation of global structure
- Hyperparameters:
  - `n_neighbours`: Balance of the local and global structure
  - `min_dist`: Controls lower dimensional projection

UMAP - 6D APOGEE

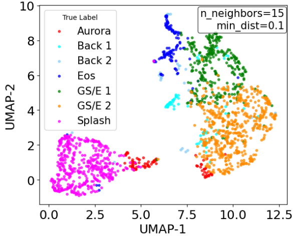

a) Colors based on High Dimensional XD

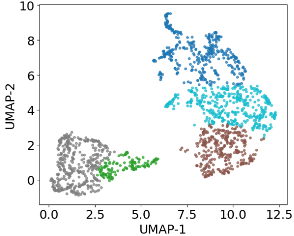

b) Colors based on GMM recovery

GS/E Eos Aurora Splash

Key Results:

- Proof of concept
- A split in Aurora?
- GMM used to demonstrate cohesion and isolation
- Caveated:
  - Non-Linear Reduction: GMM has no probabilistic foundation.

UMAP - 12D GALAH

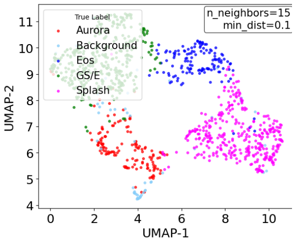

a) Colors based on High Dimensional XD

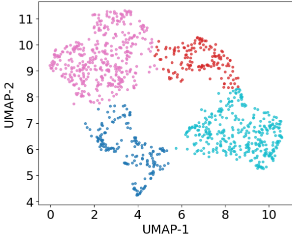

b) Colors based on GMM recovery

GS/E Eos Aurora Splash

Key Results:

- Near ‘perfect’ GMM recovery
- Greater Cohesion and Isolation:
  - 12D $\rightarrow$ Nucleosythetic discrimination
  - Is this the only reason ?

UMAP - 6D GALAH

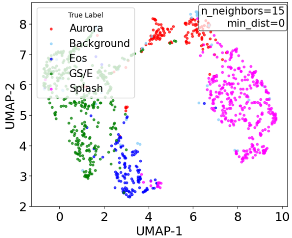

a) Colors based on High Dimensional XD

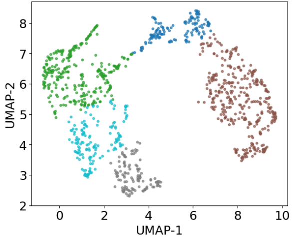

b) Colors based on GMM recovery

GS/E Eos Aurora Splash

Key Results:

- Still Greater Cohesion and Isolation
- Attributed to:
  - Exclusion of low metalicity
  - Region of ‘confusion’ with GS/E

Scalable Methodologies

A Low-Dimensional Pipeline:

1. Dimensionality Reduction
2. Clustering in Embedding Space
3. Re-projection back into Original Space

Caveat:

- Lack uncertainties in embedding space $\rightarrow$ Traditional GMM
- Approximate De-convolution of Variances:

$$\mathbf{\Sigma}_{\text{intr}} = \mathbf{\Sigma}_{\text{obs}} - \langle \mathbf{\Delta} \rangle \tag{9}$$

4 Component Re-identification

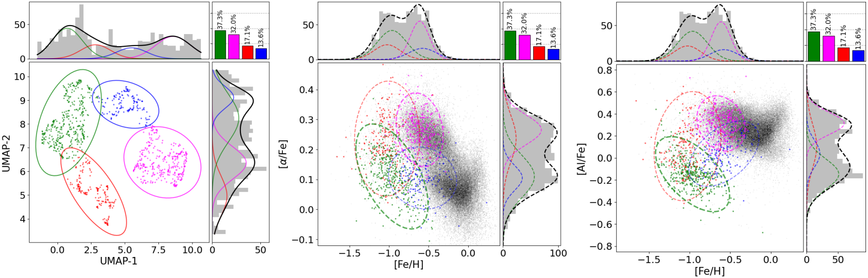

- 4.7 hours $\rightarrow$ 7 seconds (2500 $\times$ Speed-Up)
- Entirely Consistent Results
- 29.3% Increase in Uncertainties

6 Component Re-identification

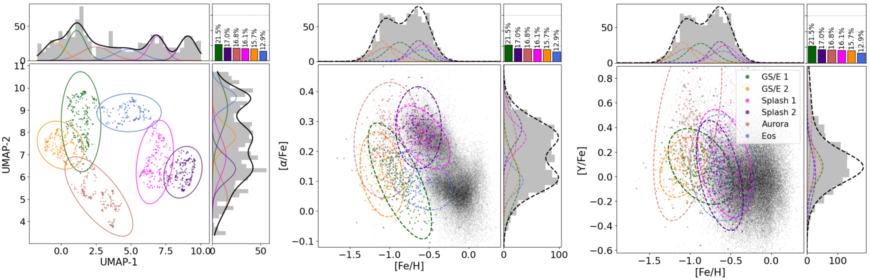

- A rough recovery of the GS/E Split
- Not achievable in high dimensional clustering

6 Component Re-identification

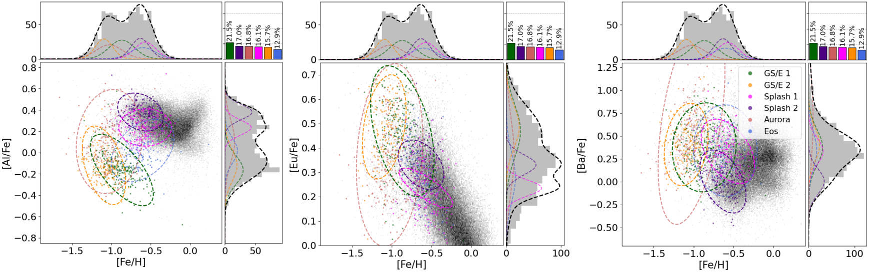

- A potential split in splash?
- A simple division of a large components in embedding space
- Or ... an astrophysical distinction

Key Results

1. **Recovered key populations:** Confirming objectivity and reproducibility.
2. **GALAH's higher dimensionality:** Provides greater halo substructure separation despite higher uncertainties.
3. **Clustering in Embedding space:**
   - Near-identical results to high-dimensional analysis
   - Achieved in 0.04% of the time (29% higher uncertainty)
   - A future stable and scalable alternative

Future Work

1. **Aurora's Split:** Test for bimodality in Aurora structure
2. **Splash's Split:** Explore physical basis for two Splash subpopulations (simulations)
3. **Hybrid Pipeline:**
   - Fast (low-D) clustering for initial grouping
   - Uncertainty-aware (high-D) clustering for accuracy

Questions

Thank you for your attention!

Jacob Tutt
Department of Physics, University of Cambridge
jlt67@cam.ac.uk
https://github.com/jacobtutt

APOGEE Results

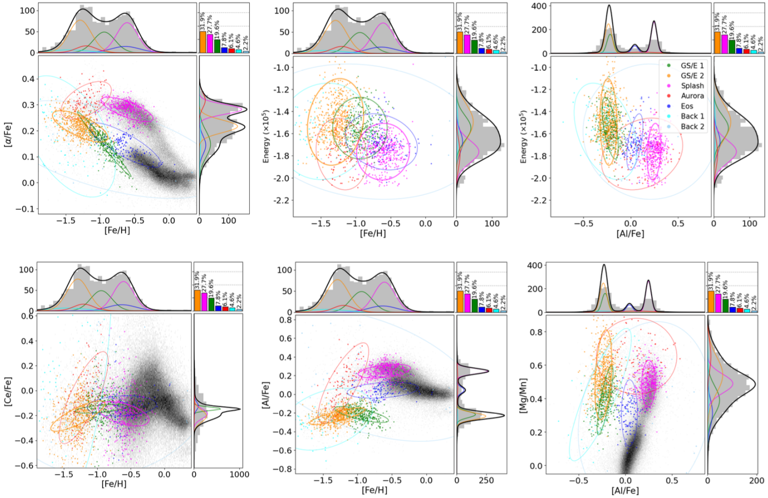

GALAH Results

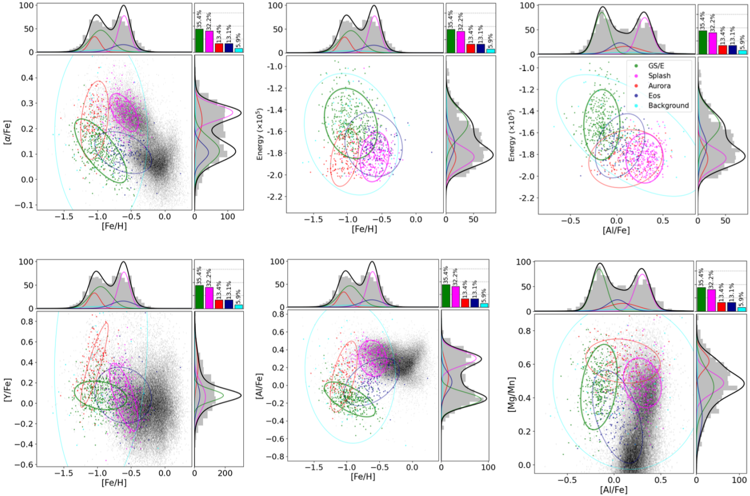

Extreme Deconvolution

Expectation-step

$$q_{ij} = \frac{\alpha_j \mathcal{N}(\mathbf{w}_i \mid \mathbf{m}_j, \mathbf{T}_{ij})}{\sum_k \alpha_k \mathcal{N}(\mathbf{w}_i \mid \mathbf{m}_k, \mathbf{T}_{ik})} \quad (10)$$

$$\mathbf{b}_{ij} = \mathbf{m}_j + \mathbf{V}_j \mathbf{T}_{ij}^{-1}(\mathbf{w}_i - \mathbf{m}_j) \quad (11)$$

$$\mathbf{B}_{ij} = \mathbf{V}_j - \mathbf{V}_j \mathbf{T}_{ij}^{-1} \mathbf{V}_j \quad (12)$$

Maximisation-step

$$\alpha_j = \frac{1}{N} \sum_i q_{ij} \quad (13)$$

$$\mathbf{m}_j = \frac{1}{q_j} \sum_i q_{ij} \mathbf{b}_{ij} \quad (14)$$

$$\mathbf{V}_j = \frac{1}{q_j} \sum_i q_{ij} \left[(\mathbf{m}_j - \mathbf{b}_{ij})(\mathbf{m}_j - \mathbf{b}_{ij})^\top + \mathbf{B}_{ij} \right] \quad (15)$$

Model Comparison

Akaike Information Criterion

- Favors models with best predictive accuracy

Bayesian Information Criterion

- Favors models with best overall fit

$$\mathrm{AIC} = 2k - 2\ln\mathcal{L},$$
$$\mathrm{BIC} = k\ln n - 2\ln\mathcal{L},$$

where:

- k: number of free parameters,
- n: number of data points,
- $\mathcal{L}$: maximum likelihood of the model.

UMAP Algorithm:

1. **Compute local distances**
   - For each point, find distance to the n-th nearest neighbor (n_neighbours)
2. **Construct Representation**
   - Build a weighted graph representing connection probabilities
   - Done using local radii (scaled by nth nearest neighbor)
   - Ensures mutual relationships are captured
3. **Optimise low-dimensional embedding**
   - Initialise points in low-dimensional space (`min_dist`)

UMAP Visualisation

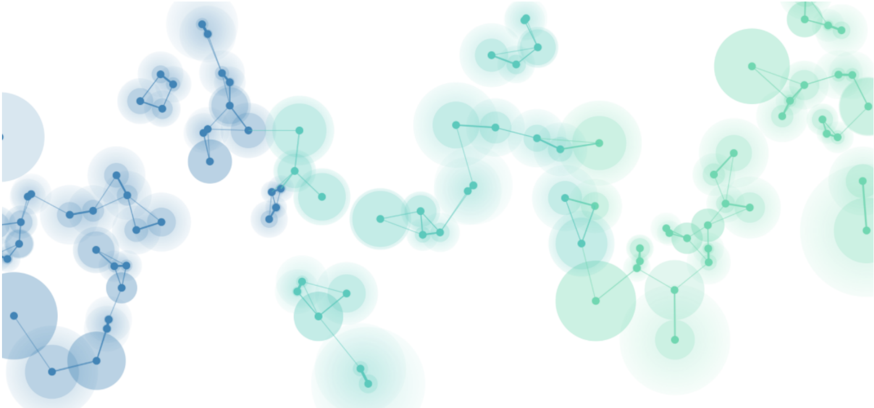

Splash Decomposition

Feature	Splash 1	Splash 2	Tracer
Colour	Magenta	Purple	
Fraction	16.1%	17.0%	
[Eu/Fe]	Lower	Higher	r-process
[Al/Fe]	Lower	Higher	Core-collapse SN
[Ba/Fe]	Higher	Lower	s-process (AGB)

Table: Comparison of chemical properties between Splash 1 and Splash 2 populations.